

NASA TECHNICAL MEMORANDUM 102719

EVALUATION OF SEVERAL MICROMECHANICS MODELS FOR DISCONTINUOUSLY REINFORCED METAL MATRIX COMPOSITES

W. S. Johnson and M. J. Birt

September 1990



National Aeronautics and
Space Administration

Langley Research Center
Hampton, Virginia 23665-5225

(NASA-TM-102719) EVALUATION OF SEVERAL
MICROMECHANICS MODELS FOR DISCONTINUOUSLY
REINFORCED METAL MATRIX COMPOSITES (NASA)
32 p C S C L 20K

N90-28872

Unclass
0304017

63/39



A Comparison of Some Micromechanics Models for Discontinuously Reinforced Metal Matrix Composites

by W. S. Johnson¹ and M. J. Birt²
NASA Langley Research Center
Hampton, Virginia

ABSTRACT

A systematic experimental evaluation of whisker and particulate reinforced aluminum matrix composites was conducted to assess the variation in tensile properties with reinforcement type, volume fraction, and specimen thickness. Each material was evaluated in three thicknesses, 1.8, 3.18, and 6.35 mm, to determine the size, distribution, and orientation of the reinforcements. This information was used to evaluate several micromechanics models that predict composite moduli. The longitudinal and transverse moduli were predicted for 15 v/o SiC_p reinforced aluminum and for 15 and 30 v/o SiC_w reinforced aluminum. The Paul model, the Cox model and the Halpin-Tsai model were evaluated. The Paul model gave a good upper bound prediction for the particulate reinforced composites but under predicted whisker reinforced composite moduli. The Cox model gave good moduli predictions for the whisker reinforcement, but was too low for the particulate. The Halpin-Tsai model gave good results for both whisker and particulate reinforced composites. An approach using a trigonometric projection of whisker length to predict the fiber contribution to the modulus in the longitudinal and transverse directions was compared to the more conventional lamination theory approach.

KEYWORDS: Aluminum matrix, silicon-carbide particulate, silicon-carbide whiskers, microstructure, moduli

Discontinuously reinforced metal matrix composites (DMMC) have been studied since the late 1970's. The most popular of these materials have been the silicon-carbide particulate (SiC_p) and the silicon-carbide whisker (SiC_w) reinforced aluminums. These materials

¹Senior Research Engineer.

²National Research Council Resident Research Associate.

exhibit significant increases in stiffness and ultimate strength over monolithic aluminum alloys. However, these composite materials have low strains to failure and very low fracture toughness values, thus limiting their applications on man-rated vehicles. Considerable research is still underway to optimize the reinforcement, material purity, and processing to improve the toughness without sacrificing the strength and stiffness. Other recent work has been in the area of developing dispersion-strengthened (XD) aluminum and titanium materials. Both of these material systems have enhanced stiffnesses and strengths due to the reinforcement and second phase particles. In all these cases metallurgists and material scientists try various combinations of reinforcement and processing to make new materials and then experimentally test the material to see if the properties are improved. It would be of great benefit to the materials development process if micromechanics models were available to help understand a priori the effect of changes in the material microstructure on the composite's mechanical properties.

Birt and Johnson [1] recently completed a study that related observed microstructural details to measured tensile properties. This study resulted in a detailed description of the reinforcement size and orientation as a function of reinforcement percentage and plate thickness. Both SiC_p and SiC_w reinforced aluminum alloy were analyzed. This paper will examine several existing micromechanical approaches for predicting composite moduli based upon the microstructural detail presented in ref. [1].

MATERIALS, TESTING AND MICROSTRUCTURE

This section will briefly summarize some of the relevant background information from the earlier report by Birt and Johnson [1]. The materials investigated were obtained both with and without reinforcement from the Advanced Composite Materials Corp. (ACMC), Greer, SC. The unreinforced matrix alloy was 2009 aluminum produced by powder metallurgy with a nominal composition of 4.0% Cu, 1.4% Mg, 0.02% Fe, bal. Al. The composites contained either 15 (actual measured and used for calculation is 15.4) volume percent (v/o) SiC_p or 15 or 30 (actual measured and used for calculation is 15.8 and 30.8, resp.) v/o SiC_w . The particulate was produced from single crystals of abrasive α -SiC that had been crushed into powder and sieved. The dimensions of the particulate were typically less than 1 μm . The whiskers were a complex mixture of α and β -SiC grown from rice hulls and designated F-9 by ACMC. The whiskers had an average diameter (d) of 0.5 μm . The whisker length prior to mixing with the prealloyed matrix powder could be as long as 60 μm . Nominally the whiskers contain a mixture of 80% whiskers and 20% broken whisker debris. For example, in the text the 15 v/o SiC_w reinforcement is really 12 v/o whiskers and 3 v/o debris. The Young's moduli of the whisker and particulate were assumed to be 483 GPa [2] and 410 GPa [3], respectively.

Four materials were produced: Unreinforced matrix alloy, 15 and 30 v/o whisker reinforced composites, and 15 v/o reinforced particulate composites. Each material type was obtained in three plate

thicknesses, 6.35 mm, 3.18 mm, and 1.8 mm, and were rolled from the same billet. More details on plate manufacturing and specimen preparation are found in Ref. [1].

Tensile property data were obtained from two duplicate tests of materials in the as-fabricated condition. The test specimens were cut from each plate of material in the L-T and T-L orientations. All tests were conducted in laboratory air at room temperature. Elastic modulus, proportional limit, Poisson's ratio, and ultimate tensile strength were determined for the longitudinal and transverse directions for each material type and thickness. The micromechanics models to be addressed here in will be used to predict the measured moduli.

The previous study [1] found that the microstructures of the composite materials were inhomogeneous and consisted of fine grains of matrix alloy interspersed with the SiC reinforcements to produce unevenly distributed bands of SiC. As the materials were hot-rolled to thinner plates, the banding was progressively reduced. The results obtained from image analysis of the whisker MMC's are presented in a condensed form in figures 1 and 2 [1]. We considered several increments in which to group whisker orientation. The 15° segments were chosen because smaller increments (i.e. 10°) did not change the predicted moduli significantly. Practically all the whiskers were oriented in the plane of the plate. The average whisker lengths in both the MMC's dropped with decreasing plate thickness due to whisker breakage during the rolling process. The whiskers tend to be shorter in the 30 v/o SiC_w

MMC's for a given plate thickness due to the likelihood of increased contact between the brittle whiskers causing breakage (as the processing parameters were assumed to be constant in both cases).

The image analysis data on particle size obtained for the L-T plane of the SiC_p MMC's are presented in figure 3. These results show a similar trend to those of the whiskers indicating that the particulates were also broken-up by the rolling process. The average aspect ratio (L/d) of the particulates for both the L-T and T-L directions was in the range of 1-2. Further details of the microstructures can be found in ref. [1].

Since all of the composite materials were made with the same matrix and were processed to the same plate thicknesses, the differences in tensile properties can be attributed to the effect of the reinforcement type and volume fraction. This set of material data is well suited to evaluate micromechanical models as the microstructure is the only significant variable between the sets of materials.

MICROMECHANICS MODELS

The microstructural data given in Figs. 1 and 2 indicate that the average whisker length in the SiC_w MMC results in L/d ratios between 18 and 31, with the whiskers in the thicker plates having the larger L/d ratios ($d=0.5\mu\text{m}$ for the whiskers). These L/d ratios are sufficiently large to allow fully effective load transfer by shear into the

whiskers, thus, these whiskers will fully contribute to the composite strength and stiffness. Therefore, it is appropriate to use a micromechanics model that accounts for shear load transfer into a discontinuous fiber. One such model is that proposed by Cox [4,5]. On the other hand, particles found in the SiC_p composite have an L/d ratio of approximately 1-2. This reinforcement could not be effective through a shear load transfer mechanism, but must rely upon load being introduced through the ends of the particulate. Paul [6] presented a strength of materials approach for calculating the stiffness contribution of cube-shaped particles. Lastly, the widely used Halpin-Tsai equations [7] will be evaluated as to their applicability to these particulate and whisker reinforced composites.

The Cox Model

Cox [4] developed a model for approximating the stress distributions along the fiber length for a discontinuous fiber embedded in a matrix under tensile loading as shown in Fig. 4. Cox further derived an expression for the Young's modulus in the direction of aligned parallel fibers. This model was summarized by Kelly [5] in the following equations:

$$E = E_w V_w [1 - (\tanh(\beta L/2)) / (\beta L/2)] + E_m (1 - V_w)$$

$$\text{where } \beta = [H / (E_w \pi r_o^2)]^{1/2}$$

$$H = 2\pi G_m / \ln[1 / (V_w^{1/2})]$$

$$E_w = \text{Young's modulus of the whisker}$$

E_m = Young's modulus of the matrix material

G_m = Shear modulus of the matrix material

V_w = Volume fraction of whiskers

L = Average whisker length

r_o = Average whisker radius

Cox also derived similar equations to calculate the shear and axial stress distributions along the fiber length:

$$\tau = E_w \epsilon \left(\frac{G_m}{2 E_w \ln(V_w^{-1/2})} \right)^{1/2} \sinh \beta((L/2)-x) / \cosh \beta L/2$$

$$\sigma = E_w \epsilon \left(1 - \frac{\cosh \beta((L/2)-x)}{\cosh \beta L/2} \right)$$

where ϵ = overall composite strain.

The Paul Model

Paul [6] presented a simple strength of materials approximation for the composite modulus for a cube-shaped inclusion. The basic assumptions are that the inclusion is of finite length; and the matrix and inclusion are subjected to the same strain and have the same Poisson's ratios. Paul's equation may be written as:

$$E_{11} = E_{22} = E_m [E_m + (E_p - E_m) V_p^{2/3}] / [E_m + (E_p - E_m) V_p^{2/3} (1 - V_p^{1/3})].$$

where E_m = Young's modulus of the matrix material

E_p = Young's modulus of the particulate material

V_p = Volume fraction of the particulates

Since a cube-shaped inclusion is assumed, the equation is not a function of the aspect ratio of the particulate or its specific dimensions. Thus, if particulates are broken during mechanical working, this equation will still predict the same modulus since the particulate volume fraction would remain the same.

The Halpin-Tsai Model

The Halpin-Tsai model [7] was originally developed to predict the longitudinal and transverse moduli and the associated shear moduli and Poisson's ratios of continuous fiber reinforced composites. The model equations developed for predicting the transverse modulus of the composite accounted for different fiber cross sectional shapes and packing geometry. The equations used in this study were formulated for fibers packed in a diamond array with rectangular cross sections. We will use these equations to predict the longitudinal modulus of aligned discontinuous fibers even though the model was intended to be used for the transverse modulus of continuous fibers. Reference [8] gives an example of the equations being used in such a manner.

The following set of equations were used to calculate the modulus in the longitudinal fiber direction:

$$E = E_m (1 + \xi \eta V_f) / (1 - \eta V_f)$$

where

$$\eta = [(E_f/E_m) - 1] / [(E_f/E_m) + \xi]$$

$$\xi = 2 (L/d)$$

E = Composite Young's modulus (E_{11} , E_{22})

E_f = Fiber modulus

E_m = Matrix modulus

V_f = Fiber volume fraction

L = Fiber length

d = Fiber diameter or thickness

Lamination Theory

The transverse and longitudinal moduli of the composites were calculated using lamination theory (second order tensor transformation). Lamina properties, E_{11} , E_{22} , G_{12} , and ν_{12} , are required. In this case the longitudinal modulus of a unidirectional whisker-reinforced composite, E_{11} , was calculated using either the Cox or Halpin-Tsai model. The transverse moduli, E_{22} , (assuming the 90° whiskers could be treated as particulates with an aspect ratio of 1.0) were estimated using the predictions of the Paul model, the Halpin-Tsai model, and available experimental data on the particulate reinforced MMC. The full percentage of reinforcement (0.15 or 0.30) was used for estimating the value of E_{22} . The shear moduli and Poisson's ratios were estimated by the following rule of mixtures equations of Halpin-Tsai [8,9] based on the material properties given in Table 1:

$$G_{12} = G_m G_f / (V_m G_f + V_f G_m)$$

$$\nu_{12} = V_m \nu_m + V_f \nu_f$$

The values of E_{11} , E_{22} , G_{12} , and ν_{12} were used as lamina properties in a laminate program. The composite was then considered to be a six ply symmetric lay-up. Each ply was considered to be oriented at the mean angle of one of the six 15° segments previously mentioned (i.e. 7.5° , 22.5° , 37.5° , 52.5° , 67.5° , and 82.5°). The thickness of each laminate was assumed to be unity, with the thickness of each ply proportional to the percentage of whiskers contained within each of the segment. The longitudinal and transverse laminate moduli were calculated.

Calculating Modulus Using Whisker Projected Lengths

The longitudinal and transverse moduli (E_{11} and E_{22}) were also calculated using a trigonometric projection of the average whisker lengths based on the observed microstructural details. This approach is less rigorous than lamination theory, however, the authors wished to assess it's applicability to whisker reinforced composites. The average whisker length for the particular plate thickness being analyzed was projected in the longitudinal and transverse direction for each of the mean angles 7.5° , 22.5° , 37.5° , 52.5° , 67.5° , and 82.5° for the six 15° segments. The fiber volume fraction in the longitudinal and transverse direction was modified by the ratio of the projected fiber lengths to the actual fiber length. The projected average whisker lengths and the modified fiber volume fraction were then used

to calculate the transverse and longitudinal moduli for each 15° segment using either the Cox or Halpin-Tsai model described earlier. A rule of mixtures was used to calculate the overall composite modulus as follows: the longitudinal and transverse moduli calculated for each of the six segments were multiplied by the modified volume fraction of whiskers in that particular segment orientation. These products were then summed in the longitudinal and transverse directions to give the composite E_{11} and E_{22} moduli.

PREDICTIONS

The predictions for the matrix properties that account for the presence of the debris will be presented first. The predictions for the particulate reinforced composites will follow. Lastly, the predictions for the whisker reinforced composites will be presented and discussed.

Properties of Matrix Material Containing Debris

As previously mentioned, the reinforcement contained approximately 20% debris. This debris had very low aspect ratios, in the order of one to two, but could still serve to stiffen the matrix material.

Therefore, the matrix was modeled as a particle (debris) stiffened composite. The properties of the stiffened matrix (G , E , and ν) were calculated using the Halpin-Tsai equations given above. Table 1 gives the assumed mechanical properties of the matrix and whisker. The debris was assumed to have the same properties as the whisker. Table 2

gives the calculated properties of the debris reinforced matrix for both the 15 and 30v/o whisker reinforced material. V_d is the assumed debris volume fraction for the matrix material. These calculated matrix properties were used in the calculations of E_{11} and E_{22} for the whisker reinforced composites.

Particulate Reinforced Composite Predictions

Figure 5 shows the predictions of the longitudinal and transverse moduli of the 15 v/o SiC_p material using the Halpin-Tsai, Cox, and the Paul models. There is only one value of moduli for the Paul model because it does not account for the reinforcement aspect ratio being slightly different for each orientation and plate thickness. However, this one value is in very good agreement with both the transverse and longitudinal moduli of the 3.18 mm and 6.25 mm plate thickness. The Halpin-Tsai model predictions correlate quite well. The Cox model predicts composite moduli which are lower than even the matrix modulus. This is due to the fact that the Cox model introduces load into the fiber through shear transfer only. Thus the fibers with low aspect ratios will not be efficient. (This will be discussed further in the next section.) Indeed, for this model prediction, the particulate was even less efficient than the matrix material. Therefore the Cox model should not be used for predicting the moduli of particulate reinforced composites.

Whisker Reinforced Composites

The whisker reinforcements of the composites contain nominally 80% whisker and 20% broken whisker debris. For the following predictions, the modulus of the matrix material was modified to account for the stiffness increase due to the debris (Table 2) as previously discussed. Therefore, the actual percentage of whiskers used for calculating the composite moduli was 0.1264 and 0.2464 for the 0.158 and 0.308 volume fraction of reinforcement, respectively.

The longer the whisker the more effective is its load carrying capacity. The Cox model [4] was used to predict the axial stress distributions along the length of whiskers of varying length as shown in Figure 6. This figure clearly shows that the longer the whisker the more effective is the load carrying capacity. The figure shows that below the $10\mu\text{m}$ whisker length, the maximum stress attained in the whisker decreases. Above $10\mu\text{m}$ whisker length, the maximum attainable stress does not increase significantly but the length of the whisker that supports the maximum stress does increase. The figure also shows the stress distribution along a short whisker with an aspect ratio of 2:1 ($1\mu\text{m}$). According to the Cox model calculation, this short whisker is extremely ineffective because the load is introduced into the whisker by shear transfer only. This explains the low predicted modulus of the particulate reinforced MMC discussed earlier using the Cox model.

Figures 7 through 10 compare the predicted moduli for the whisker reinforced plates to the experimental data. The predicted moduli are given for the Halpin-Tsai and Cox models on each figure where both the trigometric projections of whisker length and the lamination theory were used. No approach is clearly superior. For the 15 v/o whisker material, the Cox model with the trigometric projections looks the best. For the 30 v/o whisker material, the lamination theory approach is generally low and the trigometric projection is on the high side. The worst prediction was the Halpin-Tsai predictions using trigometric projections for the 30 v/o whisker material with the thick plate and that prediction was less than 15% too high. This agreement is quite good considering that the measured microstructural properties were read directly into rather simple models with no material specific empirical correction factors. The main reason for the good correlation is that the microstructural details, i.e. whisker size and orientation, were very well characterized.

In order to assess the significance of accurate whisker orientation data, the composite moduli were calculated assuming (a) that all of the whiskers were aligned in the loading direction and (b) that the whisker alignment was random. Figures 11 and 12 show the predictions for the Cox model with trigometric projections for the measured whisker orientations, totally aligned and totally random. From these figures one can see the possible extreme values of a 15 v/o whisker reinforced composite. The accurate orientation information allowed for accurate predictions of the moduli.

SUMMARY

A systematic experimental evaluation of whisker and particulate reinforced aluminum matrix composites was reported in Ref. [1] which assessed how the tensile properties varied with reinforcement type, volume fraction, and plate thickness. In addition to the tensile properties, each plate of material was analyzed to determine the size, distribution, and orientation of the reinforcements. That information was used in this study as input to several simple micromechanics models to assess their predictive capability. The longitudinal and transverse moduli were predicted for the 15 v/o SiC_p reinforced aluminum and for the 15 and 30 v/o SiC_w reinforced aluminum. Each composite material was evaluated in three thicknesses: 1.8, 3.18, and 6.35 mm.

The Paul model is a "strength of materials" estimate of the material stiffness. The particular form of the Paul Model that was evaluated was derived for a cube shaped inclusion. The Paul model gave a reasonable upper bound prediction of the particulate composite modulus but was not appropriate for the whisker reinforced materials.

The Cox model appeared to give the best predictions overall for the whisker reinforced materials. The Cox model was also used to calculate the shear and axial stress distribution along the whisker length. However, since this model only accounts for reinforcement load transfer through shear, it cannot accurately predict the moduli of short fiber ($L/d \leq 4$) or particulate reinforced composites.

The Halpin-Tsai model was evaluated because it gave an acceptable estimate of the Young's Modulus for each of the composite systems studied. The load transfer mechanism is significantly different between the whisker and the particulate; the former induces load into the fiber through shear transfer while the latter is more of an inclusion problem with a strength of materials local load transfer mechanism. Therefore, it is somewhat surprising that the Halpin-Tsai predictions correlate so well with data for both the particulate and whisker reinforced composites.

Trigonometric projections of whisker lengths were used to predict the fiber modulus contribution in the longitudinal and transverse directions and were compared to the more conventional lamination theory approach (second order tensor transformation.) In this comparison there was no clearly superior approach. The predictions were different. In some cases one approach gave results closer to the experimental data and vice versa. The trigonometric projection approach always predicted moduli values that were higher than those predicted by the lamination theory. In all cases the predictions were within 15% of the experimental data.

Given a good microstructural characterization of the composite material, several micromechanics models and analysis approaches proved capable of giving good predictions of composite moduli. However, the user must be aware that some of the models have limitations as to the type of reinforcement they are best suited to analyze.

ACKNOWLEDGEMENT

The second author, Michael Birt, gratefully acknowledges the support extended by the National Research Council, Washington D.C., through their Associateship Program.

REFERENCES

- [1] Birt, M. J. and Johnson, W. S., "Characterization of the Tensile and Microstructural Properties of an Aluminum Metal Matrix Composite," Fundamental Relationships Between Microstructural & Mechanical Properties of Metal Matrix Composites, TMS, Feb. 1990, pp.71-88.
- [2] Rosinger, H. E., Ritchie, I. G. and Shillinglaw, A. J., "A Systematic Study of the Room Temperature Elastic Moduli of Silicon Carbide", Materials Science Engineering, 16 (1974), pp. 143-154.
- [3] Skibo, M. D., "Stiffness and Strength of SiC-Al Composites," (Report SAND81-8212, Sandia National Laboratories, 1981).
- [4] Cox, H. L., "The Elasticity and Strength of Paper and Other Fibrous Materials," British Journal of Applied Physics, Vol 3, 1952, pp.72-79.
- [5] Kelly, A., Strong Solids, 2nd Edition, Clarendon Press, Oxford, 1973, pp. 175-182.
- [6] Paul, B., "Prediction of Elastic Constants for Multiphase Materials," Trans. Metallurgical Society of AIME, Feb. 1960, pp. 36-41.
- [7] Ashton, J. E., Halpin, J. C., and Petit, P. H., "Primer on Composite Materials: Analysis," Technomic, 1969, pp. 77-83.
- [8] Jones, R. M., Mechanics of Composite Materials, McGraw-Hill, New York, 1975.
- [9] Bahei-El-Din, Y. A., "Plastic Analysis of Metal Matrix Composite Laminates," Ph.D. thesis, Duke University, Durham, NC, July 1979.

TABLE 1 - MATERIAL PROPERTIES

MATERIAL	E, GPa	G, GPa	ν
MATRIX	72	27	0.32
WHISKER	483	206.4	0.17
PARTICULATE	410	175	0.17

TABLE 2 - MATRIX PROPERTIES ADJUSTED FOR DEBRIS CONTENT

V_f	E, GPa	G, GPa	ν	V_d
0.15	77.2	27.9	0.315	0.0362
0.30	84.2	29.1	0.308	0.0817

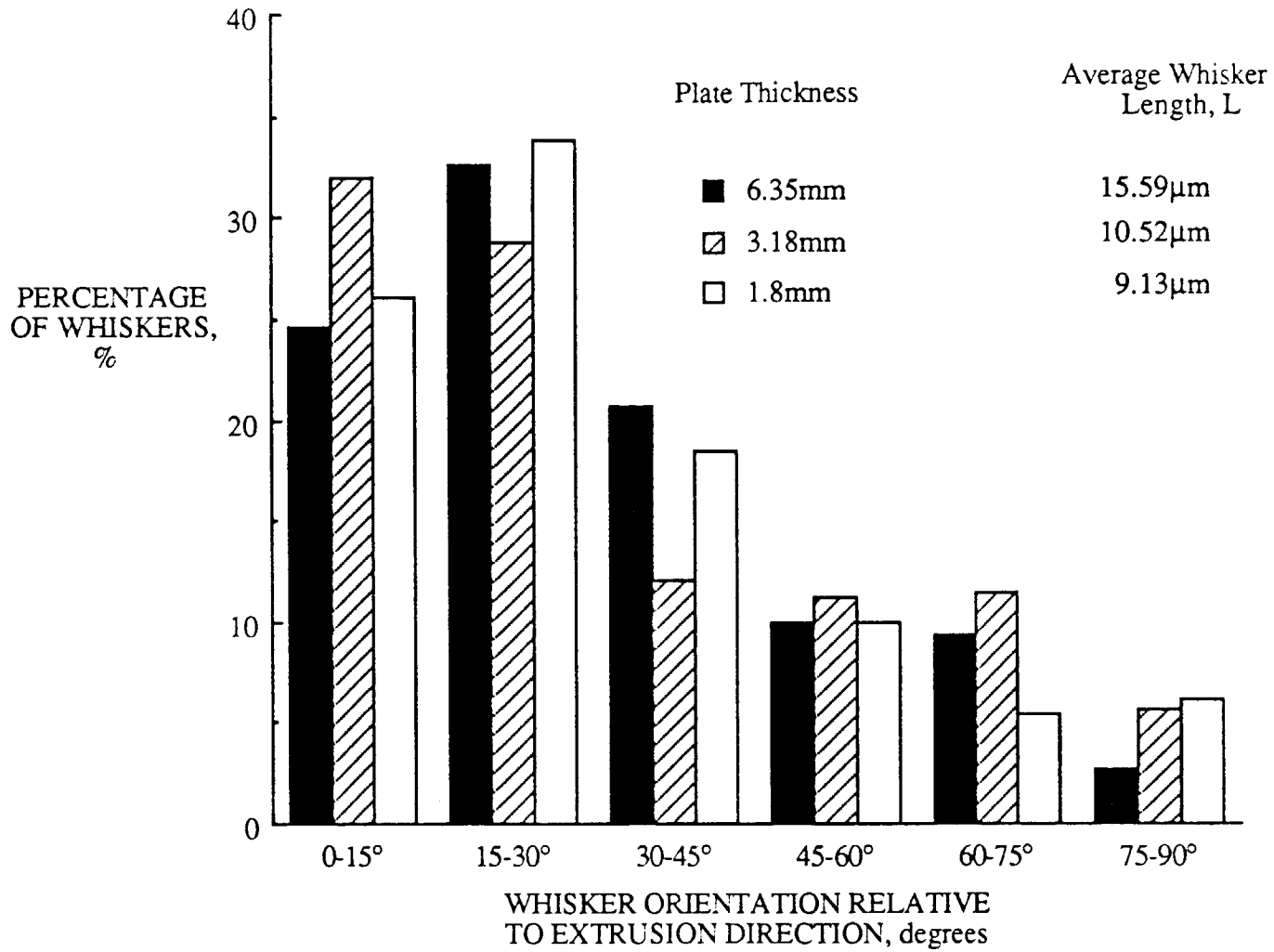


Figure 1 - Distributions of Whisker Orientations for the 15 v/o Whisker MMC.

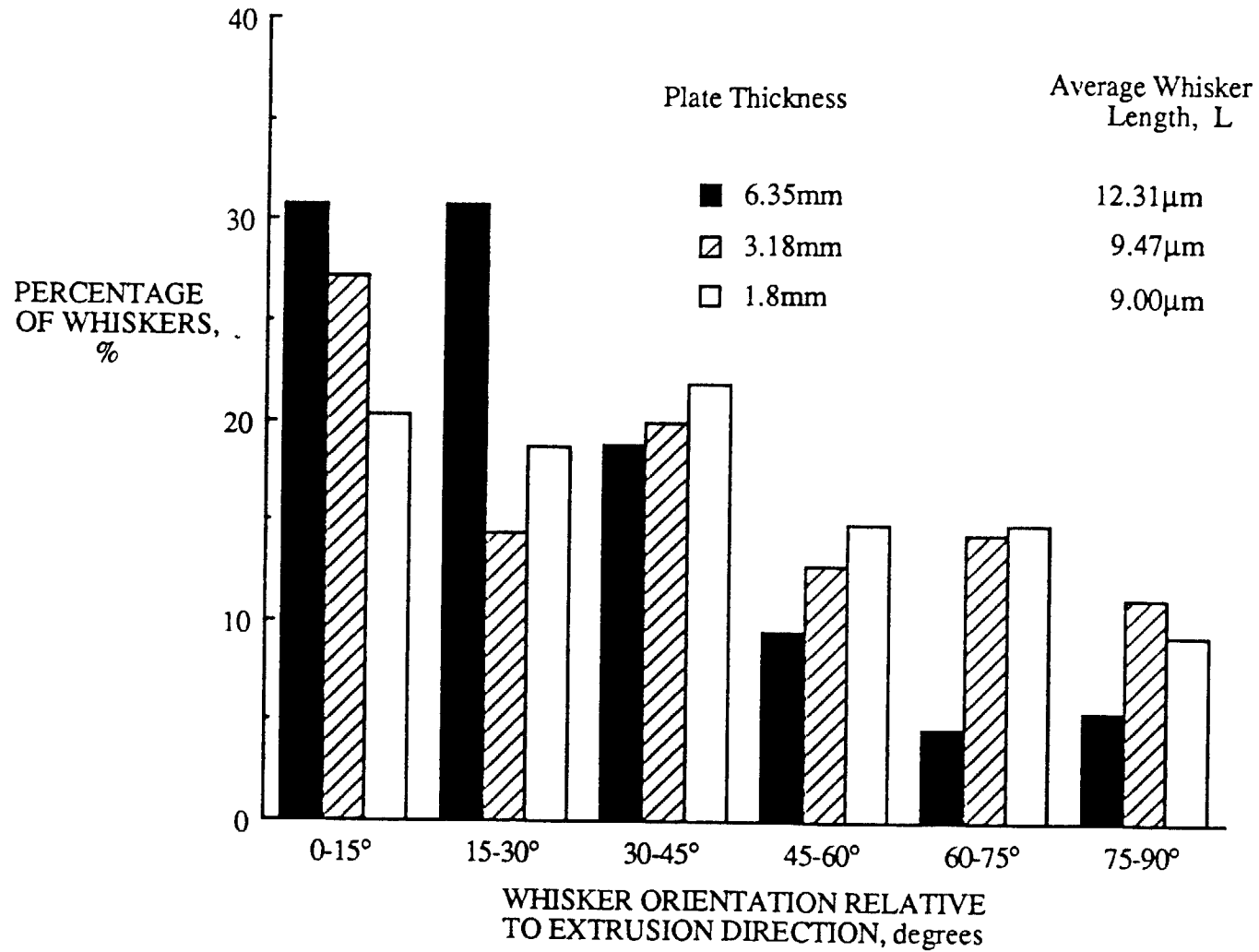


Figure 2 - Distributions of Whisker Orientations for the 30 v/o Whisker MMC.

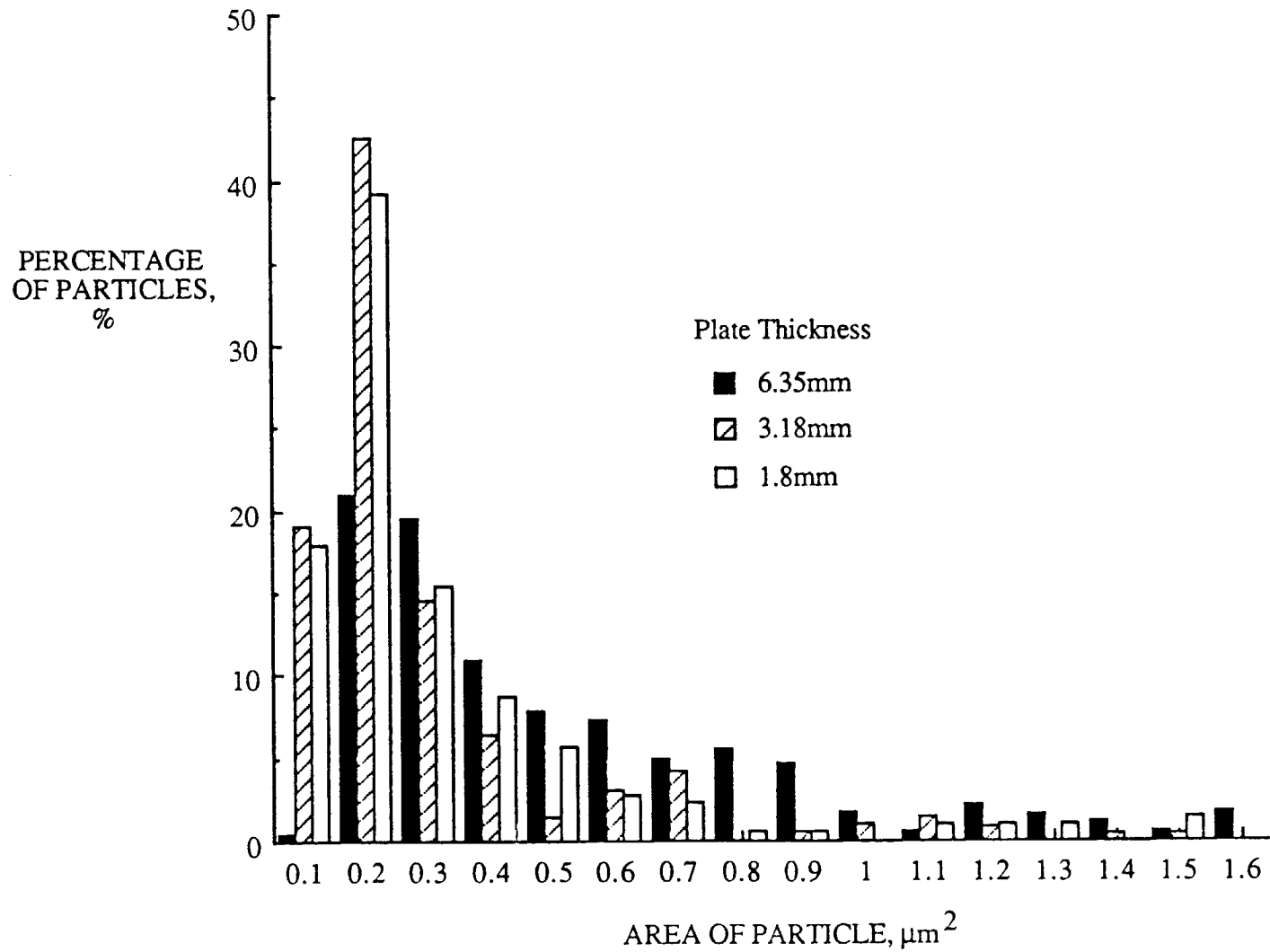


Figure 3 - Size Distributions of 15 v/o Particulate (L-T Plane)

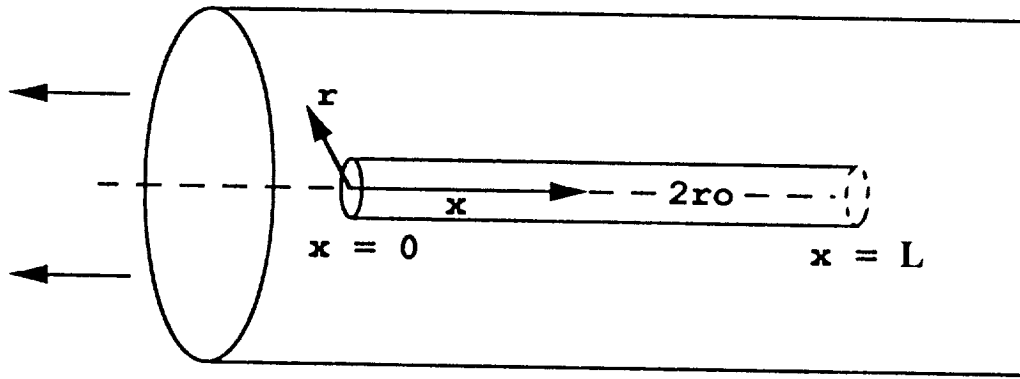


Figure 4 - Cox Embedded Short Fiber Model.

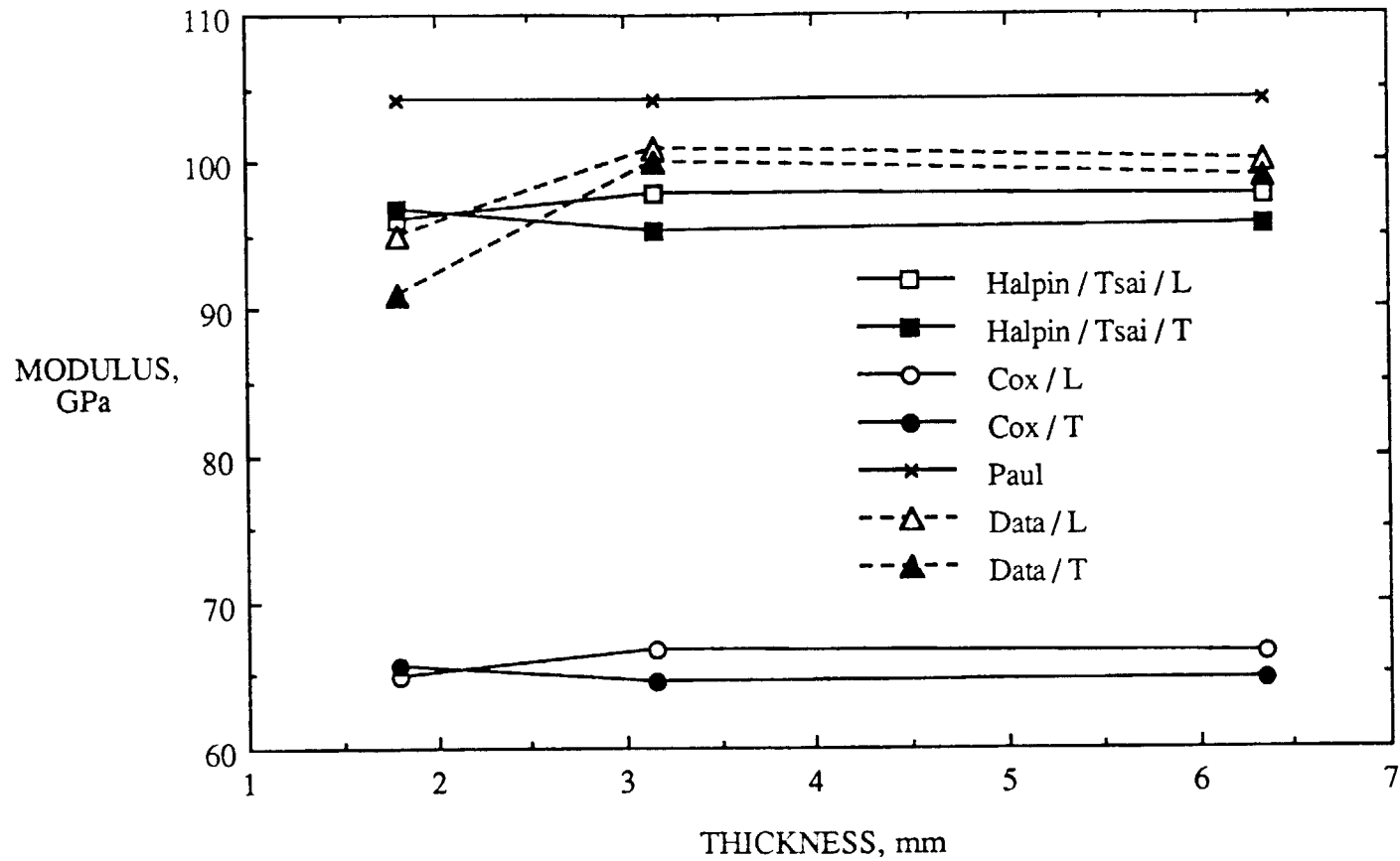


Figure 5 - Comparison of Experimental and Predicted Young's Moduli for the 15 v/o Particulate MMC (L- Longitudinal, T- Transverse Directions).

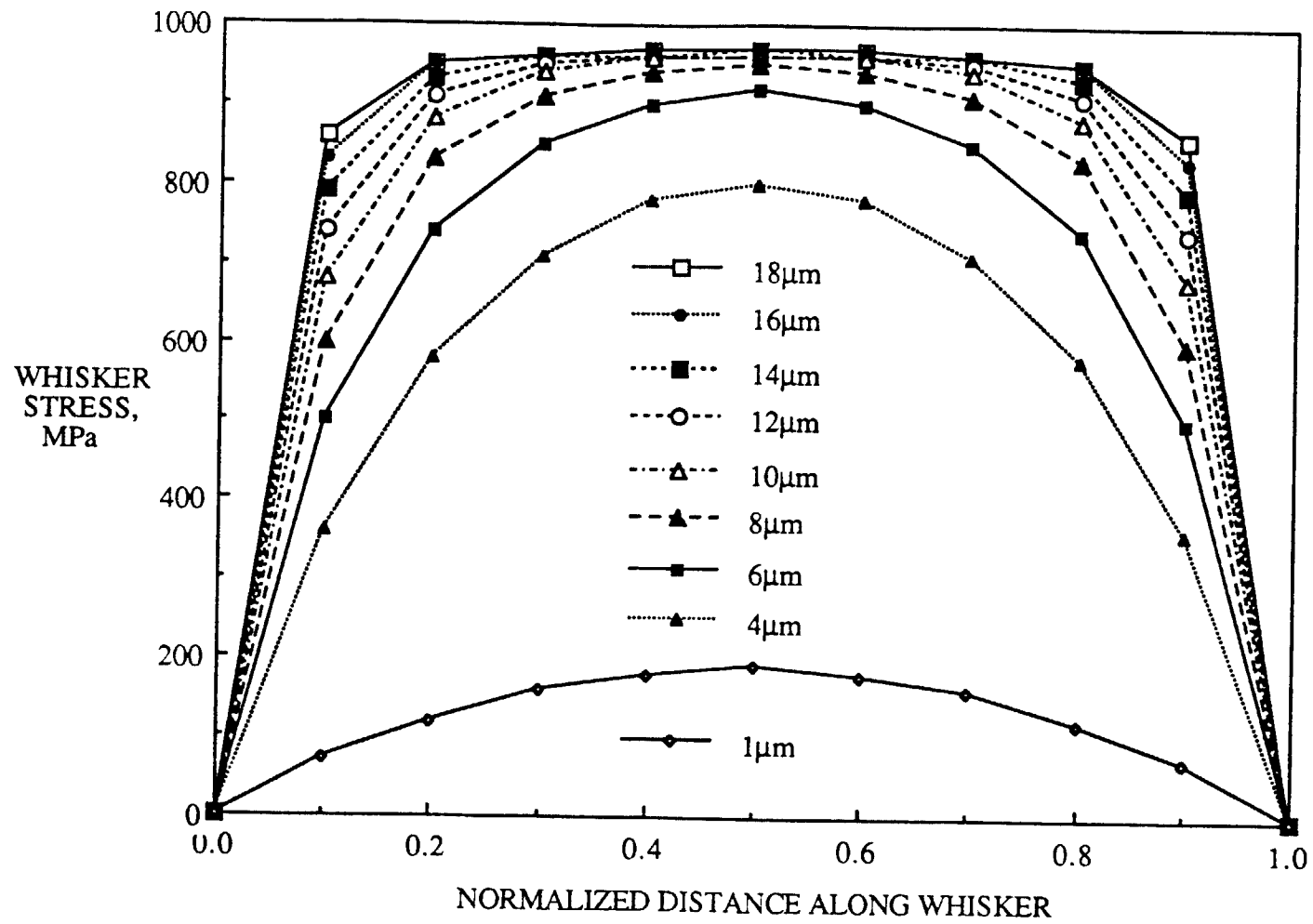


Figure 6 - Axial Stress Distribution Along a Whisker (15 v/o Whisker MMC)

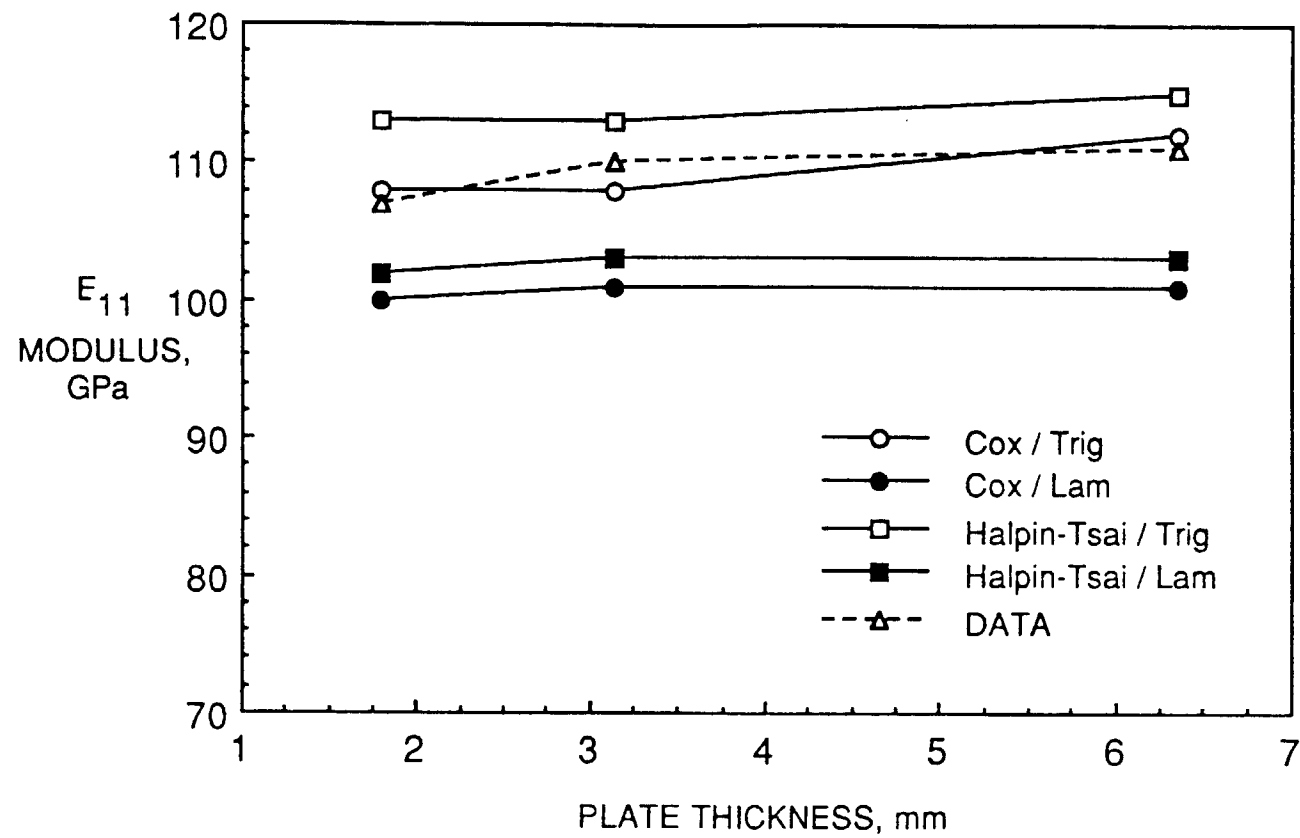


Figure 7 - Comparison of Experimental and Predicted Young's Moduli for the 15 v/o whisker MMC (Longitudinal Direction).

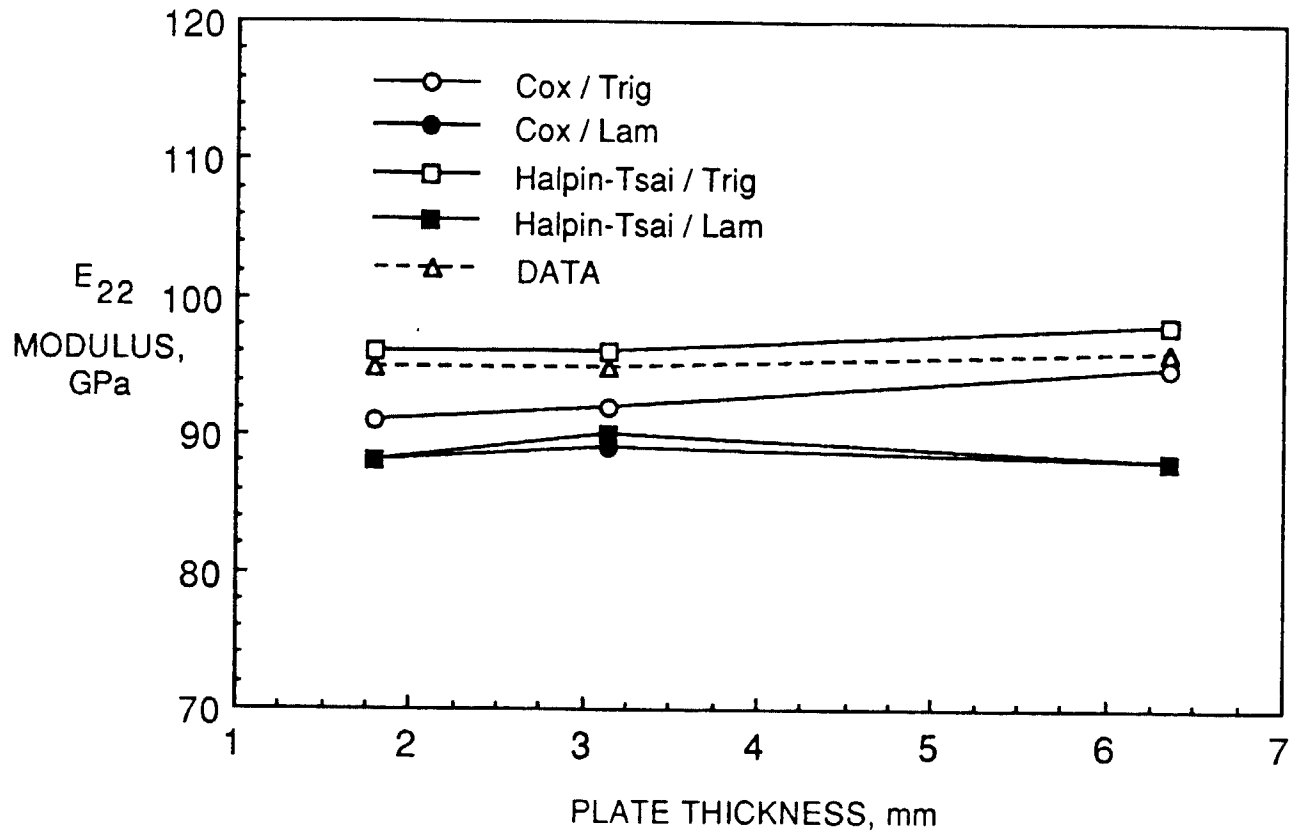


Figure 8 - Comparison of Experimental and Predicted Young's Moduli for the 15 v/o whisker MMC (Transverse Direction)

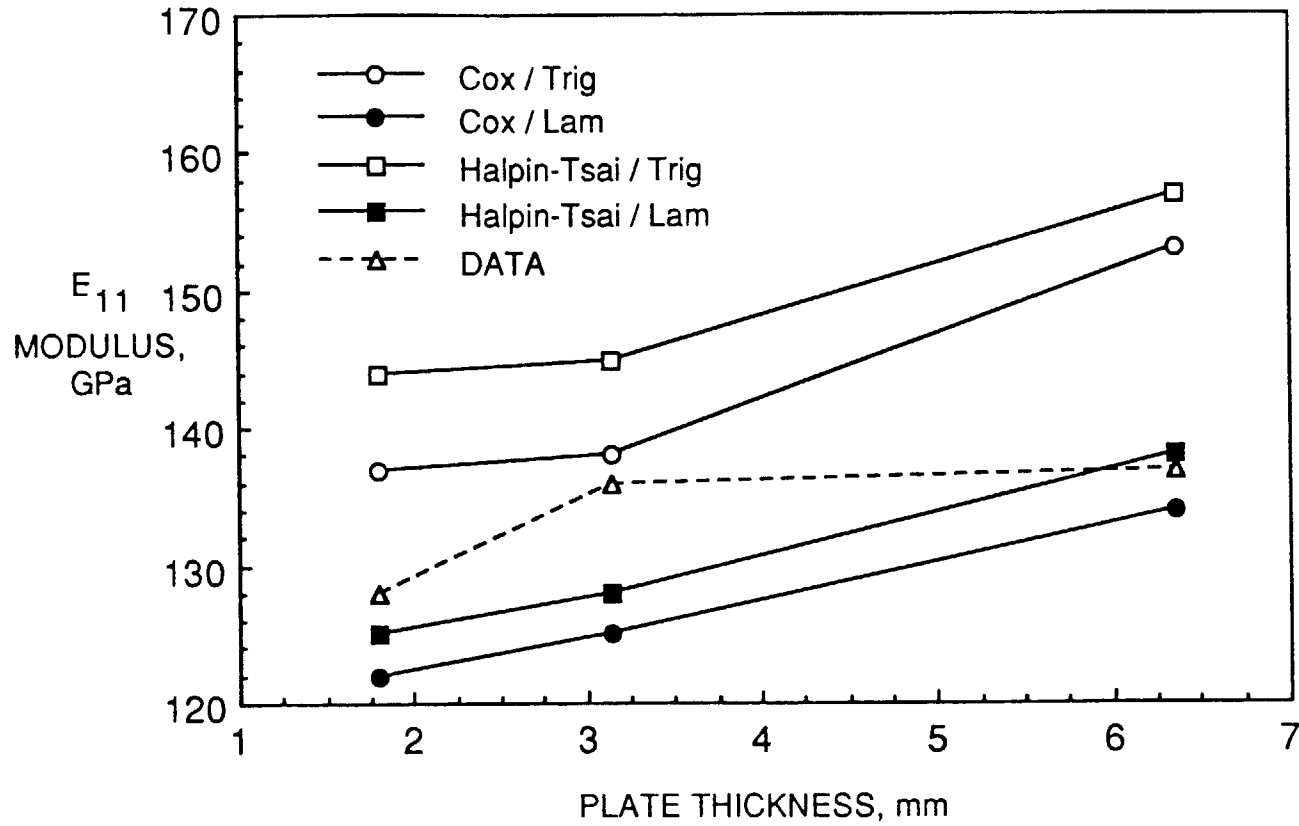


Figure 9 - Comparison of Experimental and Predicted Young's Moduli for the 30 v/o whisker MMC (Longitudinal Direction).

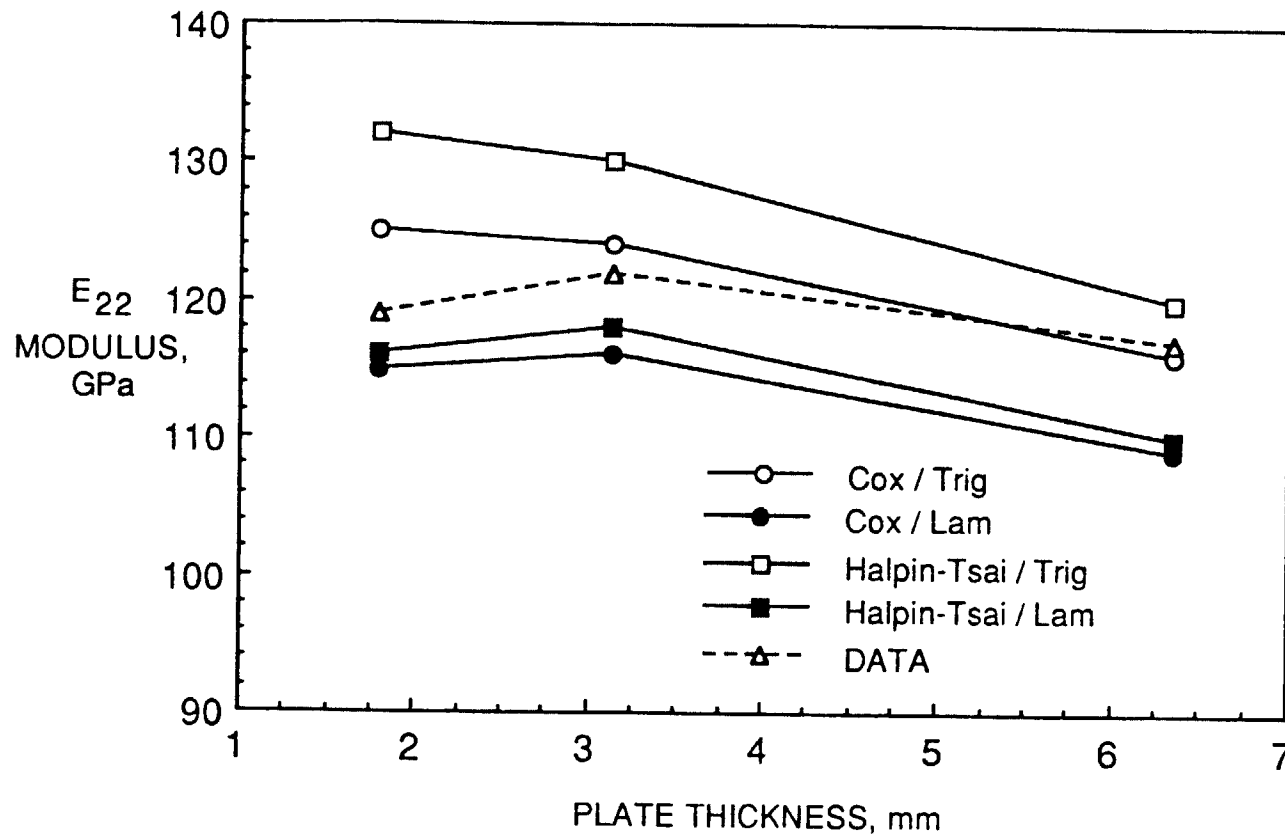


Figure 10 - Comparison of Experimental and Predicted Young's Moduli for the 30 v/o whisker MMC (Transverse Direction).

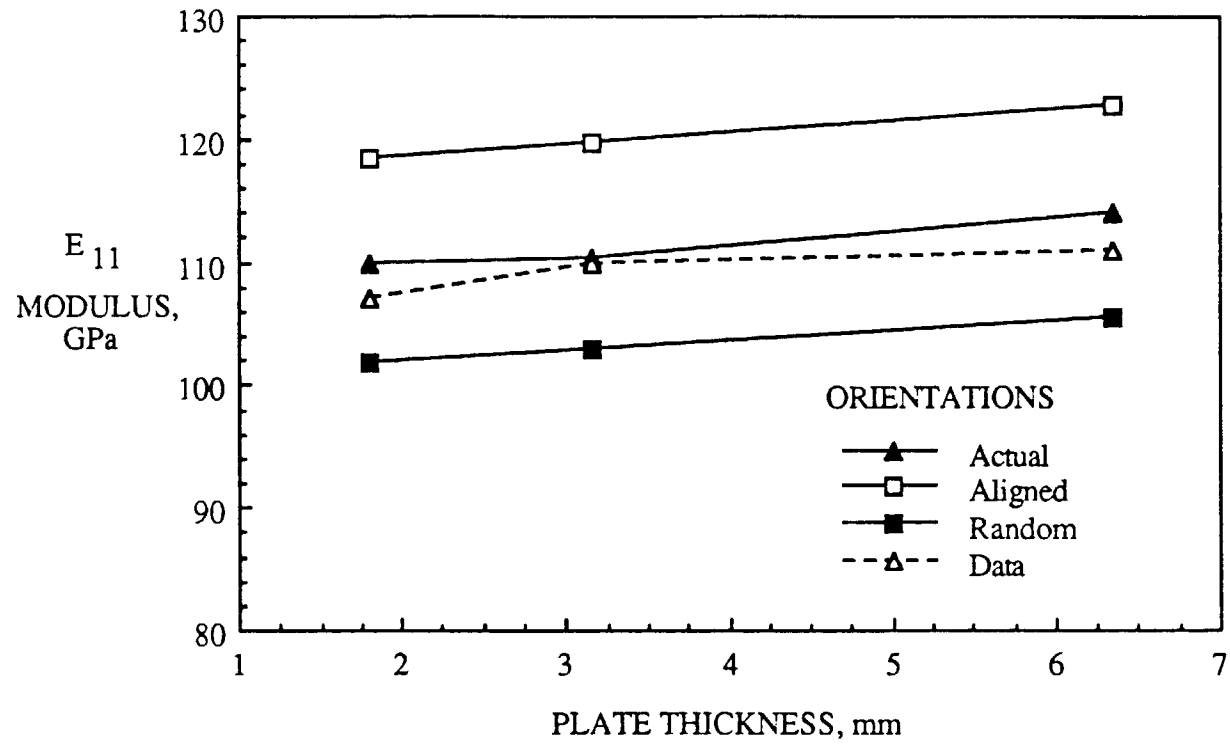


Figure 11 - Variation of Young's Moduli with Whisker Orientation for the 15 v/o whisker MMC (Longitudinal Direction)

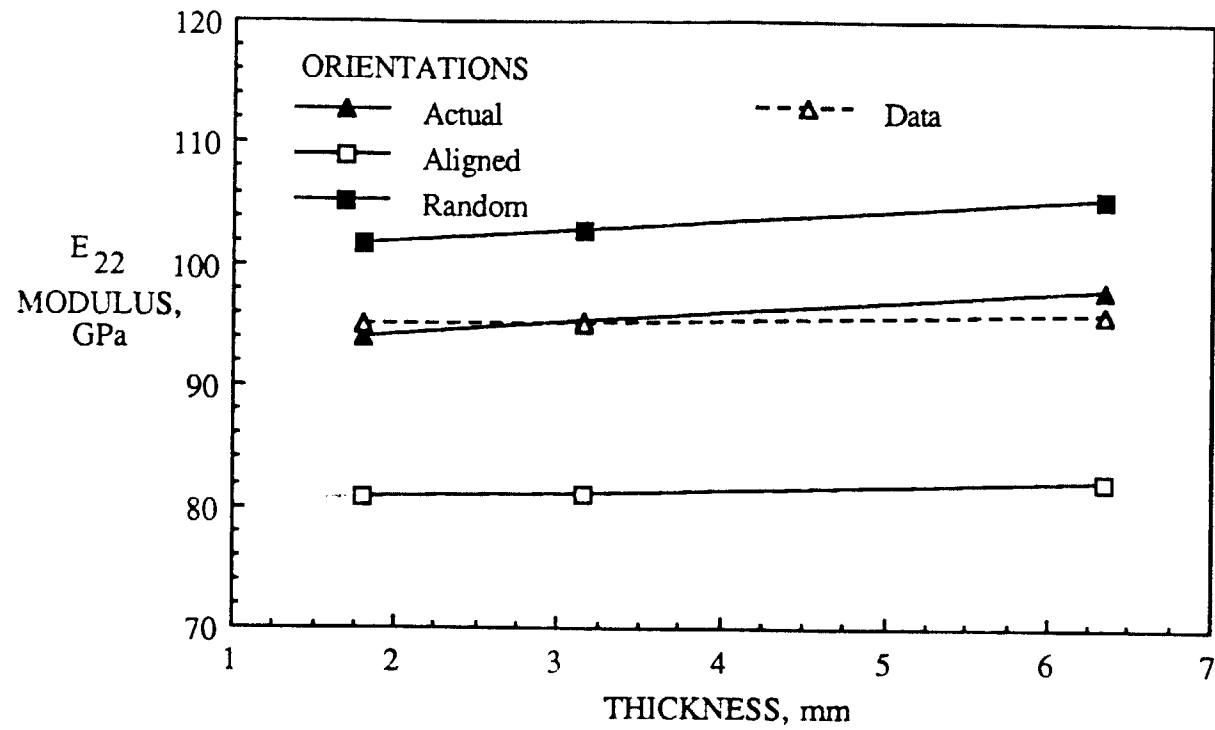


Figure 12 - Variation of Young's Moduli with Whisker Orientation for the 15 v/o whisker MMC (Transverse Direction)

